Finite-Element Analysis of Axisymmetric Cavity Resonator Using a Hybrid Edge Element Technique

Jin-Fa Lee, *Member, IEEE,* Gregory M. Wilkins and Raj Mittra, *Fellow, IEEE*

***Abstract*—A modified finite-element technique for the analysis of axisymmetric cavities is presented. In this analysis an edge element approach is used in conjunction with a nodal approach to represent all electric field components in the cavity. A bilinear functional is formulated from which resonant frequencies and/or field distributions are obtained. Several geometries are investigated and corresponding results are presented as verification of the method.**

I. Introduction

In a previous paper the authors have investigated the field behavior in coaxial geometries [1] for which the configuration was uniform in the azimuthal, or ϕ, direction and the mode of operation was also invariant in this direction. We refer to this class of problems as axisymmetric and perform the analysis using techniques suitable for two-dimensional geometries by considering any arbitrary ϕ-plane. There exists, however, a class of circularly cylindrical geometries for which the configuration is once again invariant in the azimuthal direction, but the field behavior is not independent of ϕ. For this type of problem we usually have an *a priori* knowledge of the azimuthal variation of the field behavior in the configuration and may incorporate this information into our analysis. Since the azimuthal variation is no longer considered an unknown, we may approach the problem by modifying the two-dimensional analysis to accommodate the three-dimensional problem.

The investigation of field behavior in the circular cavity resonator is an important problem in its own right. The use of the circular cavity resonator in microwave application has generated substantial interest, and both experimental and numerical research have been performed [2]–[10]. For the purposes of our investigation, we have employed a finite-element method (FEM) technique. Although in the previous investigation a nodal approach was used, implementing this type of technique to the present problem results in spurious, or nonphysical, modes. This is caused by the improper modeling of the null space of the curl operator in the conventional nodal finite-element formulation [11]. To model the null space correctly, Lee, Sun, and Cendes [12] have suggested the use of the edge-element method or the higher-order version, i.e., the tangential vector finite-element method (TVFEM). The application of the edge-element method and/or the TVFEM to study two-dimensional dielectric waveguides [12], three-dimensional MMIC passive devices [13], and three-dimensional eddy-current problems [14], has been successful and reported in the literature. In the present investigation we modify the edge-element technique for use in the modeling of axisymmetric cavities.

In the axisymmetric problems, the azimuthal direction is always tangential to the interface of material boundaries. Therefore, a straightforward extension of the edge-element approach is to use edge-elements together with nodal finite elements for modeling the transverse and the azimuthal components, respectively, of the field vector in the variational formulation. However, as will be shown in Section II, this approach does not correctly model the null space of the curl operator in the cylindrical coordinate system. As a result, spurious modes are generated. To circumvent this problem, a change of variables has also been introduced in Section III. Through this change of variables, we are able to construct a solution space that contains the null space of the discretized curl operator and consequently reduces all the spurious modes to zero eigenvalues.

In the remainder of this paper we present an overview of the generalized axisymmetric problem. In Section II, a brief discussion on the null space of the curl operator is presented. A new and reliable vector finite-element formulation for modeling axisymmetric field problems is proposed in Section III. Several numerical results are presented in Section IV to confirm the validity of the current approach. Also presented in Section IV is a convergence study demonstrating second-order accuracy in the eigenvalues obtained using the new method. Finally, a brief conclusion is presented in Section V.

II. Null Space of the Curl Operator

In the cylindrical coordinate system, the curl operator can be described as

$$\vec{\nabla}\times\vec{E}=\frac{1}{\rho}\begin{bmatrix}\hat{\rho} & \rho\hat{\phi} & \hat{z}\\ \frac{\partial}{\partial\rho} & -jm & \frac{\partial}{\partial z}\\ \boldsymbol{E}_\rho & \rho\boldsymbol{E}_\phi & \boldsymbol{E}_z\end{bmatrix}=\begin{bmatrix}\frac{1}{\rho}\left(-jmE_z-\frac{\partial}{\partial z}[\rho E_\phi]\right)\\ \frac{\partial}{\partial z}E_\rho-\frac{\partial}{\partial\rho}E_z\\ \frac{1}{\rho}\left(\frac{\partial}{\partial\rho}[\rho E_\phi]+jmE_\rho\right)\end{bmatrix}\tag{1}$$

In (1), an $e^{-jm\phi}$ dependence for every component is assumed. From (1), we see that a vector $\vec{E}^n$ is in the null space of the

Manuscript received July 16, 1991; revised February 3, 1993.

The authors are with the Electromagnetic Communication Laboratory, University of Illinois.

IEEE Log Number 9212733.

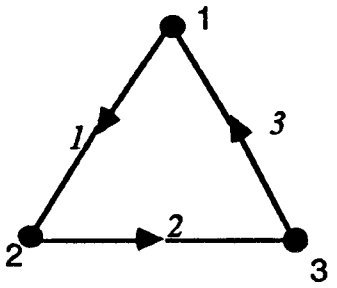

Fig. 1. Hybrid edge/nodal element.

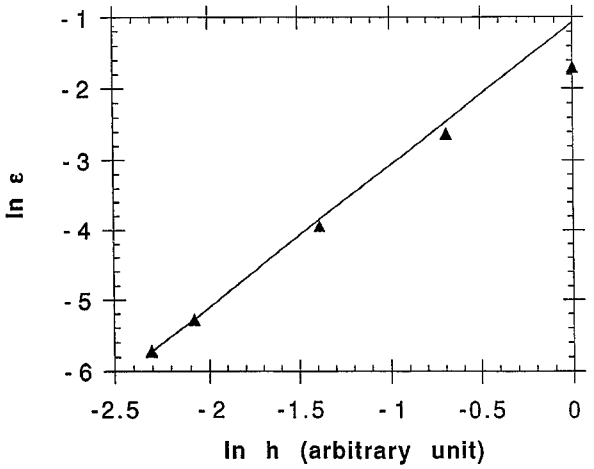

Fig. 2. Logarithmic plot of error versus relative size.

curl operator if and only if

$$jmE_z^n = -\frac{\partial}{\partial z}[\rho E_\phi^n]$$
$$\frac{\partial}{\partial z}E_\rho^n = \frac{\partial}{\partial \rho}E_z^n$$
$$jmE_\rho^n = -\frac{\partial}{\partial \rho}[\rho E_\phi^n] \tag{2}$$

In a more compact notation, we can describe the null space of the curl operator, in the cylindrical coordinate system, as

$$\Lambda_{\text{null}} = \left\{\vec{E}\,\middle|\,\left(jm\vec{E}_\tau\right) = -\vec{\nabla}_\tau(\rho E_\phi)\right\} \tag{3}$$

where

$$\vec{\nabla}_\tau = \hat{\rho}\frac{\partial}{\partial \rho} + \hat{z}\frac{\partial}{\partial z} \tag{4}$$

We note from (3) that one independent function for (ρE_ϕ) will generate one null vector. Therefore, the dimension of Λ_{null} in the discretized domain is the same as the number of degrees of freedom of the (ρE_ϕ)-component.

From (2) and (3), we see that in order to model the null space correctly in the axisymmetric formulation, the unknown variable, which is approximated by the conventional nodal scalar finite elements, should be (ρE_ϕ) instead of E_ϕ.

III. Finite Element Formulation

Beginning with Maxwells's equations

$$\vec{\nabla} \times \vec{H} = j\omega\varepsilon_r\varepsilon_0\vec{E}$$
$$\vec{\nabla} \times \vec{E} = -j\omega\mu_r\mu_0\vec{H} \tag{5}$$

TABLE I
Summary of Convergence Study

	h = 1	h = 1/2	h = 1/4	h = 1/8	h = 1/10
Number of nodes	6	15	45	153	231
Number of elements	4	16	64	256	400
Number of nodal unknowns	0	3	21	105	171
Number of edge unknowns	3	18	84	360	570
Total number of unknowns	3	21	105	465	741
Number of zero eigenvalues	0	3	21	105	171
Number of nonzero eigenvalues	3	18	84	360	570
f_0 (MHz)	13.66	12.39	11.76	11.61	11.59
Error (%)	18.26	7.27	1.82	0.52	0.35

we may obtain the vector wave equation

$$\vec{\nabla} \times \frac{1}{\mu_r}\vec{\nabla} \times \vec{E} - k_0^2\varepsilon_r\vec{E} = \vec{0} \tag{6}$$

where $k_0^2 = \omega^2\mu_0\varepsilon_0$. By using Galerkin's method [15] and assuming the cavity is made of either perfect electric or magnetic walls, we obtain the bilinear functional for the resonator problem

$$F\left(\vec{E}^c, \vec{E}\right) = \int\int_V\int\left[\left(\frac{1}{\mu_r}\vec{\nabla} \times \vec{E}^c\right)\cdot\left(\vec{\nabla} \times \vec{E}\right) - k_0^2\varepsilon_r\vec{E}^c\cdot\vec{E}\right]dV \tag{7}$$

where $\vec{E}^c$ is a testing function.

In order to accurately represent the field for any arbitrary ϕ-plane, we must decompose the field into components both transverse and normal to the plane of interest. That is, we write

$$\vec{E} = \vec{E}_\tau + \hat{\phi}E_\phi \tag{8}$$

Similarly, we define

$$\vec{\nabla} = \vec{\nabla}_\tau + \hat{\phi}\frac{1}{\rho}\frac{\partial}{\partial \phi} \tag{9}$$

Using these definitions, the bilinear functional now becomes

$$F\left(\vec{E}^c, \vec{E}\right) = \int\int_V\int\frac{1}{\mu_r}\cdot\left\{\left[\left(\vec{\nabla}_\tau \times \vec{E}_\tau^c\right)\cdot\left(\vec{\nabla}_\tau \times \vec{E}_\tau\right) + \frac{1}{\rho^2}\frac{\partial\vec{E}_\tau^c}{\partial\phi}\cdot\frac{\partial\vec{E}_\tau}{\partial\phi}\right] - \left[\frac{1}{\rho}\left(\frac{\partial\vec{E}_\tau^c}{\partial\phi}\cdot\vec{\nabla}_\tau E_\phi\right) + \frac{1}{\rho^2}\left(\hat{\rho}\cdot\frac{\partial\vec{E}_\tau^c}{\partial\phi}\right)E_\phi\right]$$

$$- \left[\frac{1}{\rho}\left(\vec{\nabla}_\tau E_\phi^c \cdot \frac{\partial \vec{E}_\tau}{\partial \phi}\right) + \frac{1}{\rho^2} E_\phi^c \left(\hat{\rho} \cdot \frac{\partial \vec{E}_\tau}{\partial \phi}\right)\right] + \left[\vec{\nabla}_\tau E_\phi^c \cdot \vec{\nabla}_\tau E_\phi + \frac{1}{\rho}\left(\hat{\rho} \cdot \vec{\nabla}_\tau E_\phi^c\right) E_\phi + \frac{1}{\rho} E_\phi^c \left(\hat{\rho} \cdot \vec{\nabla}_\tau E_\phi\right) + \frac{E_\phi^c E_\phi}{\rho^2}\right] \Bigg\} dV - k_0^2 \int\int_V \int \varepsilon_r \left(\vec{E}_\tau^c \cdot \vec{E}_\tau + E_\phi^c E_\phi\right) dV \quad (10)$$

By noting from (3) that $\vec{E}_\tau$ and $\hat{\phi} E_\phi$ are out of phase by $\frac{\pi}{2}$, we may choose

$$\vec{E}_\tau = \vec{e}_\tau \sin m\phi$$

and

$$E_\phi = \frac{e_\phi}{\rho} \cos m\phi \quad (11)$$

where $\vec{e}_\tau$ and e_ϕ are chosen to correctly model the null space of the curl operator, as discussed in Section II. Using this information and noting that $dV = \rho\, d\rho\, d\phi\, dz$, we may show

$$F(\vec{e}^{\,c}, \vec{e}\,) = \int_\Omega \int \frac{1}{\mu_r} \cdot \Bigg\{ \left[\rho\left(\vec{\nabla}_\tau \times \vec{e}_\tau^{\,c}\right) \cdot \left(\vec{\nabla}_\tau \times \vec{e}_\tau\right) + \frac{m^2}{\rho}\left(\vec{e}_\tau^{\,c} \cdot \vec{e}_\tau\right)\right] - \frac{m}{\rho}\left[\left(\vec{e}_\tau^{\,c} \cdot \vec{\nabla}_\tau e_\phi\right) + \left(\vec{\nabla}_\tau e_\phi^c \cdot \vec{e}_\tau\right)\right] + \frac{1}{\rho}\left(\vec{\nabla}_\tau e_\phi^c \cdot \vec{\nabla}_\tau e_\phi\right) \Bigg\} d\rho\, dz - k_0^2 \int\int_\Omega \varepsilon_r \left[\rho(\vec{e}_\tau^{\,c} \cdot \vec{e}_\tau) + \frac{e_\phi^c e_\phi}{\rho}\right] d\rho\, dz \quad (12)$$

which is a real generalized eigenvalue problem formulation.

The transverse components of the field may now be approximated in terms of edge unknowns and the azimuthal components in terms of the nodal unknowns (see Fig. 1). There is no inconsistency in this type of decomposition since E_ϕ is tangential to all boundary surfaces in the plane of interest and the condition that $E_\phi = 0$ on the conducting surfaces is easily satisfied. Similarly, since the edge unknowns represent the projection of the electric field onto a given edge of the triangular element, the condition that

$$\hat{t} \cdot \vec{E}_\tau = 0 \quad (13)$$

is also readily satisfied, where $\hat{t}$ is the unit vector tangential to the conductor surface. An advantage of the application of the edge element technique is that, because of the use of $\vec{E}_\tau$ as a state variable, we may, without difficulty, enforce the Dirichlet boundary condition for the electric field on the perfect conductor surfaces.

As previously mentioned in Section II, we have chosen edge-elements as the vector basis function for the transverse component. We may therefore express the electric field components are

$$\vec{e}_\tau = \sum_{m,n_{m \neq n}} V_{\tau_{mn}} \vec{W}_{mn} \quad (14)$$

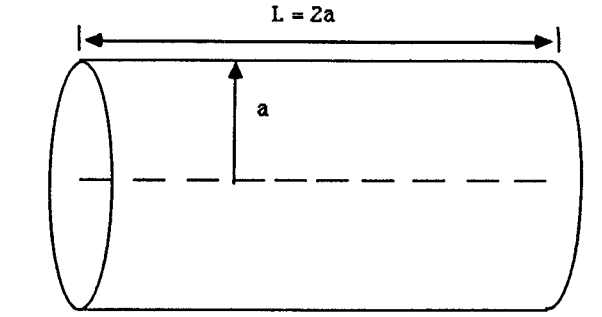

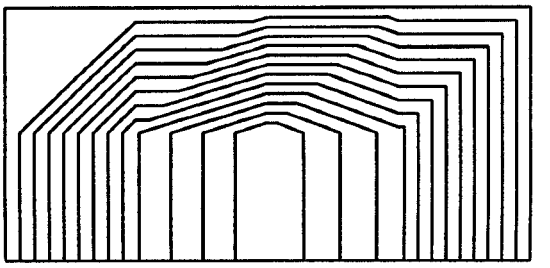

(a)

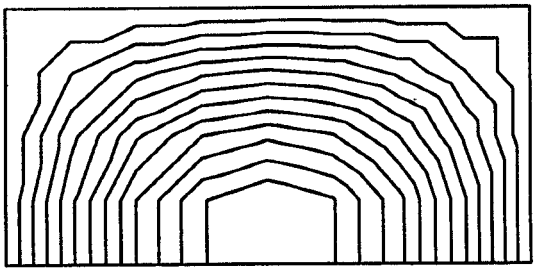

(b)

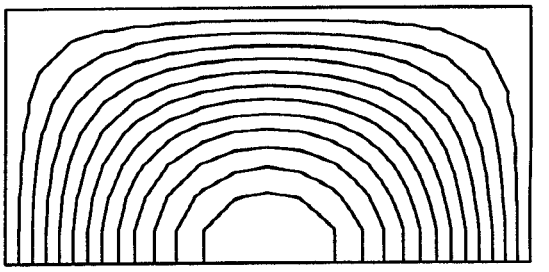

(c)

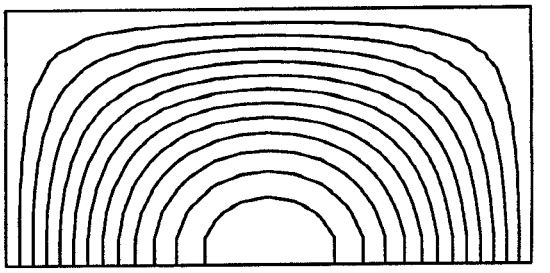

(d)

Fig. 3. Air-filled cylindrical resonator with $L = 2a$ and field patterns of azimuthal electric field component for relative sizes (a) $h = \frac{1}{2}$; (b) $h = \frac{1}{4}$; (c) $h = \frac{1}{8}$; (d) $h = \frac{1}{10}$.

and

$$e_\phi = \sum_m V_{\phi_m} \lambda_m \tag{15}$$

where $\vec{W}_{mn}$ is the vector basis function for edge $\{mn\}$ and λ_m is the first-order Lagrange interpolation polynomial for node m [16]. From our choice of $e_\phi \propto \rho E_\phi$ we see that $e_\phi \equiv 0$ at $\rho = 0$ for all azimuthal modes since E_ϕ is finite at this location. It has been noted [17], however, that while $e_z = 0$ at $\rho = 0$ for azimuthal modes $m \neq 0$, e_z has a finite nonzero value for $m = 0$ and $\vec{e}_\tau$ is subsequently treated as an unknown at the center of the cavity.

Finally, by enforcing the requirement that

$$F(\vec{e}^{\,c}, \vec{e}) = 0 \tag{16}$$

for any testing function $\vec{e}^{\,c}$ in the testing function space, we obtain the generalized eigenmatrix equation

$$[A]\underset{\sim}{e} = k_0^2 [B]\underset{\sim}{e} \tag{17}$$

where

$$\begin{aligned} \underset{\sim}{e}^T [A]\, \underset{\sim}{e} \;= \int\int_\Omega \Bigg\{ \Bigg[& \rho \left(\vec{\nabla}_\tau \times \vec{e}_\tau^{\,c}\right) \cdot \left(\vec{\nabla}_\tau \times \vec{e}_\tau\right) \\ & + \frac{m^2}{\rho} (\vec{e}_\tau^{\,c} \cdot \vec{e}_\tau) \Bigg] \\ & - \frac{m}{\rho} \left[\left(\vec{e}_\tau^{\,c} \cdot \vec{\nabla}_\tau e_\phi\right) + \left(\vec{\nabla}_\tau e_\phi^c \cdot \vec{e}_\tau\right) \right] \\ & + \frac{1}{\rho} \left(\vec{\nabla}_\tau e_\phi^c \cdot \vec{\nabla}_\tau e_\phi\right) \Bigg\} d\rho\, dz \end{aligned} \tag{18}$$

and

$$\underset{\sim}{e}^T [B] \underset{\sim}{e} = \int\int_\Omega \varepsilon_r \left[\rho (\vec{e}_\tau^{\,c} \cdot \vec{e}_\tau) + \frac{e_\phi^c e_\phi}{\rho} \right] d\rho\, dz \tag{19}$$

IV. Numerical Results

In assembling the eigensystem we notice that there are singular terms when $\rho \to 0$. A common practice is to apply a transformation of the form $F = \sqrt{\rho} f$ [18] to eliminate this singularity, where f is now the quantity to be approximated. However, an alternate approach is to utilize numerical integration techniques [15]. A seven-point numerical integration provides acceptable accuracy.

The convergence of the current method is illustrated in Fig. 2, where h represents the relative size of an individual mesh element. The test geometry is an air-filled circular cavity for which the cavity length is twice the radius and the TE_{111} mode is dominant with a resonant frequency of $f_0 = 11.55$ MHz. The convergence is governed by $\varepsilon \propto h^N$, where ε is the error relative to the exact solution [19] and N is the value to be determined, i.e., the rate of convergence. From the figure, we see that as h is decreased, the slope of the error is asymptotic to the line of slope 2, corresponding to $N = 2$, i.e., $\varepsilon \propto h^2$. Table I summarizes the convergence study.

A measure of the effectiveness of the numerical method arises from observing the field pattern. Figure 3 shows the geometry of interest and illustrates the electric field strength for the azimuthal component of the fundamental mode in the resonator. Due to the symmetry of the problem, it is necessary to perform analysis and present results for only one azimuthal plane of the geometry. The field pattern also indicates convergences as h is decreased. The patterns for the cases $h = \frac{1}{2}$, $h = \frac{1}{4}$, $h = \frac{1}{8}$, and $h = \frac{1}{10}$ are presented.

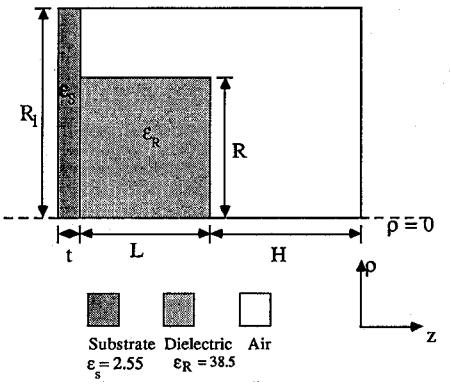

Fig. 4. Cylindrical dielectric resonator investigated by Kooi *et al.* $L = 5$ mm; $R = 6.5$ mm' $R_1 = 9.75$ mm; $t = 0.762$ mm; $H = 5$ mm.

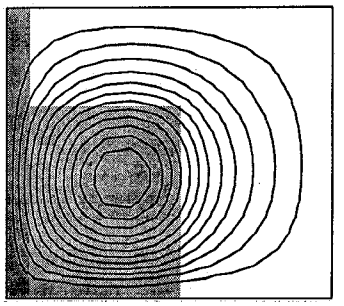

Fig. 5. Field pattern for dominant mode of resonator in Fig. 4.

A point of observation is that there is a one-to-one correspondence between the number of nodal unknowns and the number of zero eigenvalues, as suggested in Section II. This is in general true for the modes corresponding to $m > 0$, for which $\vec{e}_\tau$ and e_ϕ both vanish at $\rho = 0$. For the modes corresponding to $m = 0$, the number of zero eigenvalues exceeds the number of nodal unknowns due to the additional unknowns at $\rho = 0$. These unknowns represent the fact that, for $m = 0$, $\vec{e}_\tau$ is nonzero at the center of the cavity, while e_ϕ once again vanishes.

Several other examples are worth examining. Kooi *et al.* [8] investigate the cylindrical dielectric resonator (Fig. 4) operating in the so-called $TE_{01\delta}$ mode, where $\delta < 1$. In this problem the authors use a nodal approach since the geometry and the field are ϕ-invariant. A comparison of the resonant frequencies for the dominant mode obtained by the nodal approach versus the current method shows an agreement of approximately 3%. Figure 5 illustrates the field behavior for the dominant mode obtained by the current method.

Lebaric and Kajfez [9] use a finite integration technique to analyze the dielectric resonator cavity in Fig. 6. The finite element mesh used in the current study corresponds to 391

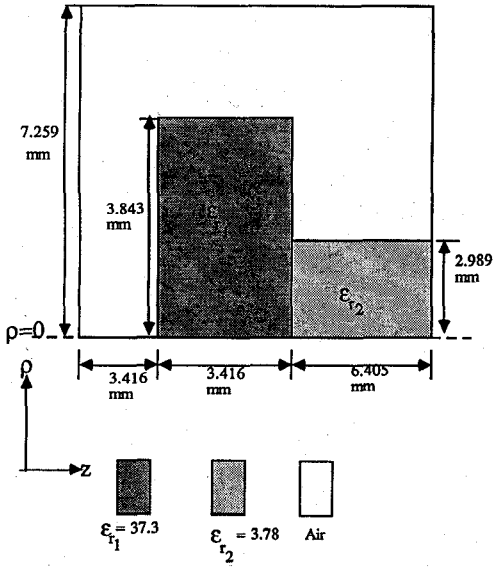

Fig. 6. Dielectric resonator cavity investigated by Lebaric and Kajfez.

TABLE II
COMPARISON OF RESONANT FREQUENCIES FOR PROBLEM INVESTIGATED BY LEBARIC AND KAJFEZ

Mode	Lebaric/Kajfez (GHz)	Lee/Wilkins/ Mittra (GHz)	Measured (GHz) Reference [9]	Error of current method with measured[9] (%)
TE_{01}	7.037	7.169	6.943	3.26
HEM_{11}	8.742	8.830	8.694	1.56
HEM_{12}	8.897	9.080	8.905	1.97
TM_{01}	9.296	9.320	9.185	1.47
HEM_{21}	10.605	10.726	10.558	1.59
TM_{02}	11.113	11.164	10.943	2.02
HEM_{13}	11.226	11.490	11.184	2.74
TE_{02}	11.391	11.766	11.316	3.98

nodes and 704 triangular elements. Table II lists a comparison of the resonant frequencies obtained by the two methods, along with the relative errors for the current method. Figure 7 is a plot of the field behavior for the azimuthal component for the dominant modes corresponding to $m = 0$, 1, and 2. Keeping with the convention of the authors, this corresponds to TE_{01}, HEM_{11}, and HEM_{21}. The first subscript represents the azimuthal mode m and the second subscript represents the position in the ascending ordering for the resonant frequencies for azimuthal mode m.

Taheri and Mirshekar-Syahkal [10] use a one-dimensional finite-element method to examine several loaded cylindrical cavities. Results and relative errors for the dielectric rod (Fig. 8) and the dielectric disk (Fig. 9) are given in Tables III and IV respectively.

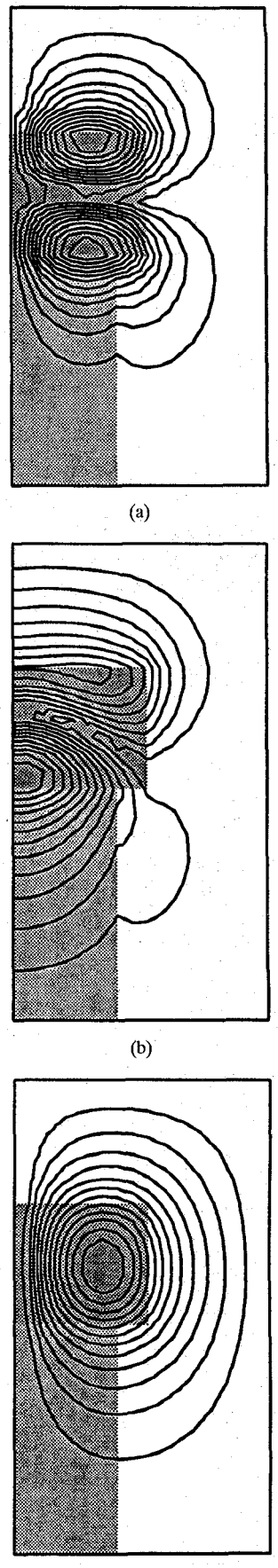

(a)

(b)

(c)

Fig. 7. Azimuthal components for dominant modes corresponding to $m = 0$, 1, and 2 for the resonator of Fig. 6.

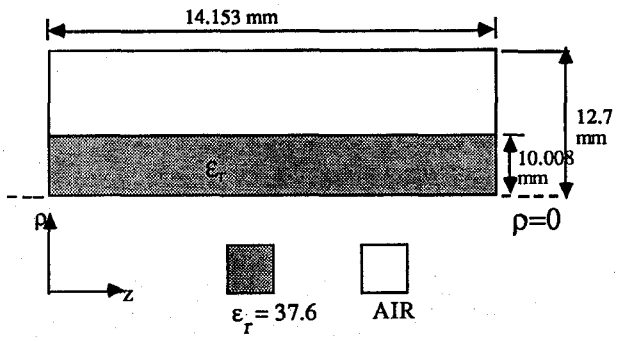

Fig. 8. Cavity loaded with dielectric rod.

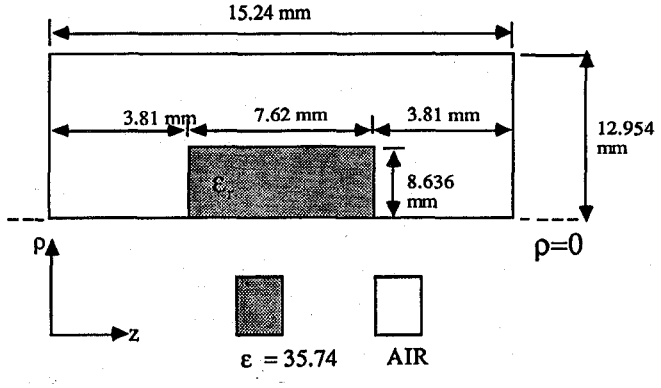

Fig. 9. Cavity loaded with dielectric disk.

TABLE III
COMPARISON OF RESONANT FREQUENCIES FOR CAVITY LOADED WITH DIELECTRIC ROD

Mode	Taheri/ Mirshekar-Syahkal (GHz)	Lee/Wilkins/ Mittra (GHz)	Measured(GHz) Reference [2]	Error of current method with measured [2] (%)
TM_{010}	Not available	1.497	1.554	3.668
HE_{111}	2.489	2.498	2.494	0.160
TE_{011}	Not available	3.059	3.108	1.577
HE_{211}	3.402	3.334	3.391	0.715
TM_{011}	3.380	3.375	3.363	0.357
HE_{121}	3.813	3.835	3.828	0.183
HE_{112}	Not available	3.895	3.828	1.75
HE_{131}	Not available	4.539	4.531	0.177

V. CONCLUSIONS

A generalized finite-element approach utilizing edge unknowns in conjunction with nodal unknowns has been presented for the analysis of axisymmetric circular cavities. The method proves to be versatile and lends itself to many applications. For instance, this approach can be modified for use in design problems that are of great interest in the development of electronic packaging techniques.

TABLE IV
COMPARISON OF RESONANT FREQUENCIES FOR CAVITY LOADED WITH DIELECTRIC DISK

Mode	Taheri/ Mirshekar-Syahkal (GHz)	Lee/Wilkins/ Mittra (GHz)	Measured (GHz) Reference [3]	Error of current method with measured[3] (%)
TE_{01}	3.435	3.508	3.428	2.334
HE_{11}	4.271	4.266	4.244	0.518
HE_{12}	4.373	4.361	4.326	0.809
TM_{01}	4.601	4.535	4.551	0.352
TE_{02}	5.493	5.462	5.592	2.325

REFERENCES

[1] G. M. Wilkins, J.-F Lee, and R. Mittra, "Numerical modeling of axisymmetric coaxial waveguide discontinuities," *IEEE Trans. Microwave Theory Tech.*, vol. MTT-39, pp. 1323–1328, Aug. 1991.

[2] K. A. Zaki and C. Chen, "Loss mechanisms in dielectric-loaded resonators," *IEEE Trans. Microwave Theory Tech.*, vol. MTT-33, pp. 1448–1452, Dec. 1985.

[3] ——, "New results in dielectric-loaded resonators,' *IEEE Trans. Microwave Theory Tech.*, vol. MTT-34, pp. 815–824, July 1986.

[4] K. A. Zaki, C. Chen, and A. E. Atia, "Canonical and longitudinal dual-mode dielectric resonator filters without iris," *IEEE Trans. Microwave Theory Tech.*, vol. MTT-35, pp. 1130–1135, Dec. 1987.

[5] K. A. Zaki and C. Chen, "Coupling of non-axially symmetric hybrid modes in dielectric resonators," *IEEE Trans. Microwave Theory Tech.*, vol. MTT-35, pp. 1135–1142, Dec. 1987.

[6] K. A. Zaki, C. Chen, and A. E. Atia, "A circuit model of probes in dual-mode cavities," *IEEE Trans. Microwave Theory Tech.*, vol. MTT-36, pp. 1740–1746, Dec. 1988.

[7] A. Navarro, M. J. Nuñez, and E. Martin, "Study of TE_0 and TM_0 modes in dielectric resonators by a finite-difference time-domain method coupled with the discrete Fourier transform," *IEEE Trans. Microwave Theory Tech.*, vol. MTT-39, pp. 14–17, January 1991.

[8] P. S. Kooi, M. S. Leong, and A. L. Satya Prakash,"Finite-element analysis of the shielded cylindrical dielectric resonator," *IEE Proc. Inst. Elec. Eng.*, vol. 132, pp. 7–16, Feb. 1985.

[9] J. E. Lebaric and D. Kajfez, "Analysis of dielectric resonator cavities using the finite integration technique," *IEEE Trans. Microwave Theory Tech.*, vol. MTT-37, pp. 1740–1748, November 1989.

[10] M. M. Taheri and D. Mirshekar-Syahkal, "Accurate determination of modes in dielectric-loaded cylindrical cavities using a one-dimensional finite element method," *IEEE Trans. Microwave Theory Tech.*, vol. MTT-37, pp. 1536–1541, Oct. 1989.

[11] S. H. Wong and Z. J. Cendes, "Combined finite element-modal solution of three-dimensional eddy current problems," *IEEE Trans. Magn.*, vol. MAG-24, pp. 2685–2687, 1988.

[12] J.-F. Lee, D.-K. Sun, and Z. J. Cendes, "Full-wave analysis of dielectric waveguides using tangential vector finite elements," *IEEE Trans. Microwave Theory Tech.*, vol. MTT-39, pp. 1262–1271, Aug. 1991.

[13] J.-F. Lee, "Analysis of passive microwave devices by using three-dimensional tangential vector finite elements," *Int. J. Numer. Modeling: Electron. Networks, Dev. Fields*, vol. 3, pp. 235–247, December 1990.

[14] A. Bossavit and J. C. Vérité, "The 'TRIFOU' code: Solving the 3-D eddy current problem by using H as a state-variable," *IEEE Trans. Magn.*, vol. MAG-19, pp. 2465–2470, June 1983.

[15] G. Strang and G. J. Fix, *An Analysis of the Finite-Element Method.* Englewood Cliffs, NJ, Prentice-Hall, 1973.

[16] A. Bossavit and I. Mayergoyz, "Edge-elements for scattering problems," *IEEE Trans. Magn.*, vol. MAG-25, pp. 2816–2821, July 1989.

[17] M. A. Morgan, S-K Chang, and K. K. Mei, "Coupled azimuthal potentials for electromagnetic field problems in inhomogeneous axially symmetric media," *IEEE Trans. Antennas Propagat.*, succinct papers, pp. 413–417, may 1977.

[18] A. Konrad, "High-order triangular finite elements for electromagnetic waves in anisotropic media," *IEEE Trans. Microwave Theory Tech.*, vol. MTT-25, pp. 353–360, May 1977.

[19] R. F. Harrington, *Time-Harmonic Electromagnetic Fields.* New York: McGraw-Hill, 1961.

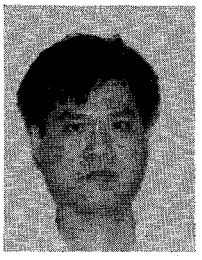

Jin-Fa Lee (M'88) was born in Taipei, Taiwan, in 1960. He received the B.S. degree from National Taiwan University, in 1982 and the M.S. and Ph.D. degrees from Carnegie-Mellon University in 1986 and 1989, respectively, all in electrical engineering.

From 1988 to 1990, he was with AnSOFT Corp., where he developed several CAD/CAE finite-element programs for modeling three-dimensional microwave and millimeter-wave circuits. From 1990 to 1991, he was a post-doctoral fellow at the University of Illinois at Urbana-Champaign. Currently, he is an Assistant Professor at Department of Electrical and Computer Engineering, Worcester Polytechnic Institute.

Dr. Lee's current research interests are analyses of numerical methods, coupling of active and passive components in high-speed electronic circuits, three-dimensional mesh generation, and nonlinear optic fiber modelings.

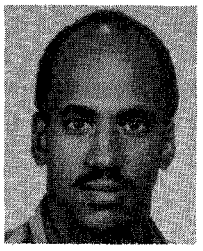

Gregory Martiné Wilkins was born in Washington D.C. on March 3, 1960. He received the B.S. degree in electrical engineering from the University of Maryland, College Park, in 1983, and the M.S. degree in electrical engineering from the Johns Hopkins University in 1984. In 1991 he completed the Ph.D. degree at the Electromagnetic Communication Laboratory at the University of Illinois at Urbana-Champaign. His research focused on the electromagnetic modeling of planar integrated circuits using various finite-element techniques. In 1991 he joined IBM Corporation in East Fishkill, New York, where he is active in advanced package design technology.

Dr. Wilkins is a member of the Tau Beta Pi Engineering Honor Society, the Eta Kappa Nu Electrical Engineering Honor Society, the National Society of Black Engineers, the American Society for Engineering Education, and the National Alumni Schools Committee of the Johns Hopkins University.

Raj Mittra (S'54–M'57–SM'69–F'71) is Director of the Electromagnetic Communication Laboratory of the Electrical and Computer Engineering Department and Research Professor of the Coordinate Science Laboratory at the University of Illinois. He is a former president of AP-S, and he has served as the editor of the IEEE TRANSACTIONS ON ANTENNAS AND PROPAGATION. He is president of RM Associates, a consulting organization providing services to several industrial and governmental organizations.

Dr. Mittra's professional interests include the areas of analytical and computer-aided electromagnetics, high-speed digital circuits, radar scattering, satellite antennas, microwave and millimeter-wave integrated circuits, frequency selective surface, EMP and EMC analysis, and remote sensing.